Desalination and Water Treatment
www.deswater.com
doi: 10.1080/19443994.2013.826399

52 (2014) 766–774
January

Taylor & Francis
Taylor & Francis Group

Novel effective waste iron oxide-coated magnetic adsorbent for phosphate adsorption

Teng Chien Chen[a,c], Gaw-Hao Huang[b], Chia-Hsun Liu[a], Chuh-Shun Chen[a], Shun-Hsing Chuang[d], Yao-Hui Huang[a,c,*]

[a]*Department of Chemical Engineering, National Cheng Kung University, Tainan 701, Taiwan*
Email: yhhuang@mail.ncku.edu.tw
[b]*Green Energy and Environment Research Laboratories, Industrial Technology Research Institute, Hsinchu City 30011, Taiwan*
[c]*Resource Recycling and Management Research Center, National Cheng Kung University, Tainan 701, Taiwan*
[d]*Department of Environmental Engineering and Management, Chaoyang University of Technology, Taichung, Taiwan*

Received 23 March 2013; Accepted 5 May 2013

ABSTRACT

The study investigates the adsorptive interactions of phosphate with fresh and modified waste iron oxide–coated magnetic materials (FOMs) in aqueous medium. The Brunauer Emmett Teller surface area of modified FOM is 274.8 m^2/g, providing extensive open adsorption sites for phosphate removal. Scanning electron microscope observations revealed that FOM has a fractured and rough surface morphology. The optimal adsorption capacity of modified FOM is 30.8 mg P/g which is better than fresh one in the pH 5. The adsorption process follows a pseudo-second-order kinetics with rate constant amounted to 4.1×10^4 and 3×10^2 g/mg h with phosphate concentration from 11.1 to 140.9 mg/l. The adsorption isotherms are fitted into the Langmuir model in which the co-relationship is 0.999 in this study. The low activation energy is obtained as 2.7 kJ/mol, which is the physisorption. The negative standard enthalpy and negative adsorption standard free energy in this study indicates that the adsorption of phosphate by the modified FOM adsorbent is exothermic and spontaneous reaction. The calculated maximum adsorption capacity is 30.8 mg P/g which was much higher than previous reported.

Keywords: Iron oxide; Magnetic; Adsorption; Phosphate; Fluidized-bed reactor Fenton

1. Introduction

Phosphorus is as an essential resource and material, which is used in large quantities in agriculture and optoelectronic industries. However, the extensive use of phosphate promotes the growth of the algae when it enters rivers or lakes. It is, therefore, a major cause of eutrophication. Some algae are toxic and can disturb the balance of organisms in

*Corresponding author.

Presented at the Fifth Annual International Conference on "Challenges in Environmental Science & Engineering—CESE 2012" Melbourne, Australia, 9–13 September 2012

water. The rapid depletion of dissolved oxygen when algae decay kills fish and other aquatic life. Hence, phosphorus has a serious impact on the lakes, rivers, and seas on which people depend [1,2].

The removal of phosphorus from wastewater has been extensively studied. Wastewater discharges from optoelectronic industries, civil, agricultural are major sources of phosphate pollution, and phosphate wastewater management is an important environmental issue [3]. Numerous phosphate removal methods, such as chemical coagulation, biological treatment, crystallization, advanced chemical precipitation, ion exchange, magnetic methods, and adsorption, have been studied in recent years [3–5]. Chemical precipitation and biological treatment have been applied extensively in industry, but high operating costs remain a serious challenge.

Adsorption solves high operation costs of chemical precipitation and biological treatment. The method of adsorption is found to be superior to the other aforementioned techniques for removing pollutants from aqueous solution in terms of both flexibility and simplicity, ease of implementation and insensitivity to toxic pollutants [6]. Adsorption capacity and efficiency are well known to depend strongly on the adsorbent material.

The use of industrial wastes or by-products for removing phosphorus has attracted considerable attention. Low-cost adsorbents include fly ash [7–10], blast furnace slag [11,12], red mud [13–15], alum sludge [16,17], and other materials [18–20].

To address sustainability issues, this investigation presents the adsorptive removal of phosphate using a waste iron oxide–coated magnetic material (FOM). This material is a disposable by-product of fluidized-bed reactor Fenton (FBR-Fenton) crystallization and can efficiently perform adsorptive fluoride removal [21]. A large specific surface area and a granular size of millimeters causes FOM to act as an efficient adsorbent, especially for the purposes of recycling.

The objective of this study is to examine the feasibility of using FOM as an adsorbent for removing phosphorus from wastewater. Two types of FOM—fresh FOM and modified FOM, which was made from NaOH, was added to the fresh FOM to adjust its pH to 12 and dried—are evaluated. The adsorption and desorption characteristics of FOM in the removal of phosphate from wastewater were evaluated in this experiment. The adsorption efficiency were evaluated by adsorption isotherms. The kinetics and desorption in the synthetic wastewater were evaluated. Such work could contribute to understanding the phosphate removal process using FOM.

2. Materials and methods

2.1. Materials

Synthetic wastewater for use in the adsorption experiments was made with concentrations of 0.37–4.52 mM-PO_4^{3-} (11.5–140.1 mg P/l), and Magnetic particles (Fe_3O_4) were prepared by co-precipitation method with waste Iron Oxide from FBC-Fenton reactor.

Fresh FOM was made from the magnetic particle, which was packed as a carrier in a 1.6 L FBR-Fenton reactor. H_2O_2 and $FeSO_4$ with a molar ratio of 2:1 were fed into the bottom of reactor continuously. The pH of the solution was controlled at around 3.5 to prevent $Fe(OH)_3$ precipitation. The height of fluidized-bed was maintained at a 50–100% bed expansion by controlling the upflow velocity of internal circulation. Fig. 1 displays the apparatus of FBC.

The modified FOM was made as follows: (1) NaOH was added to the fresh FOM to adjust its pH to 12, (2) the solution was stirred and shaken for 2 h, and (3) the FOM was rinsed with clean tap water to reduce its pH to 7 and was then dried at 105°C for 24 h.

All chemical agents, including NaCl, $NaNO_3$, Na_2SO_4 (also the standard for ion chromatography (IC) measurement), and CH_3COONa, used in the adsorption experiments that were analytical grade and purchased from Merck Co. The NaOH was industrial grade.

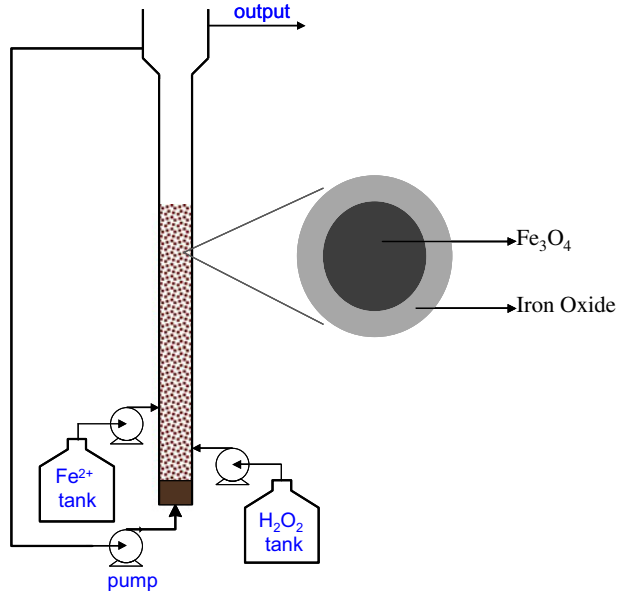

Fig. 1. The manufacture processes for fresh FOM.

2.2. Adsorption experiment

Fresh and modified iron oxide-coated materials were rinsed in clean tap water to remove ash. They were dried at room temperature. The adsorption experiments were performed in 1 L phosphate solution (0.37–4.52 mM) using jar test system and the FOMs were mixed for 72 h. The temperature and the rate of stirring were maintained at 305 K and 150 rpm, respectively. Samples were extracted and the PO_4^{3-} concentration was analyzed using IC.

2.3. Analytical methods

About 1 g FOMs sieved in the range of 26–45 μm was dissolved in 6 N HCl and identified by an atomic adsorption spectrophotometer (GBC Sens A). The Brunauer–Emmett–Teller (BET) surface area (m^2/g), micropore area (m^2/g), external surface area (m^2/g), total pore volume (cm^3/g), and adsorption average pore diameter (Å) were analyzed by a surface area/porosity analyzer (Micromeritics ASAP 2010). The micro morphology and the surface composition were examined by a scanning electron microscope (SEM; EOL JSM-6700F) and supplemented energy dispersive spectra (EDS) spectrometer (Oxford INCA-400). The crystallization of FOMs were measured by X-ray diffraction (XRD) using a counter diffractometer (Rigaku RX III) and Cu K_α radiation. The IR spectra used to detect the phosphate adsorption were obtained using a JASCO model 410 spectrometer (DRIFT, diffuse reflectance analysis mode). Anion concentrations in water samples were measured using IC (732 IC Detector, Metrohm) with a 4.6 mm i.d. × 250 mm L Metrosep A SUPP 1 column. The physical characters for fresh and modified FOMs were shown in Table 1.

Table 1
The physical characters for fresh and modified FOMs

Parameters	Fresh FOM	Modified FOM
Total iron content of catalyst (g/kg)	385	406
Bulk density (g/cm^3)	1.324	1.007
Absolute (true) density (g/cm^3)	1.953	2.509
Specific surface area (m^2/g)	240.1	274.8
Total pore volume(cm^3/g)	0.126	0.257
Average particle size (μm)	45.13	26.13

Table 2
The material elements for fresh and modified FOMs

Element	Fresh FOM		Modified FOM	
	wt.%	at.%	wt.%	at.%
C K	2.04	4.98	2.3	5.90
O K	34.51	63.34	32.44	61.35
S K	2.77	2.53	–	–
Fe L	53.33	28.04	58.49	33.71
Pt M	7.36	1.11	6.73	1.04

3. Results and discussion

3.1. Characterization of the FOM

The BET surface area of modified FOM is 274.8 m^2/g, providing extensive open adsorption sites for phosphate removal (Table 1). In the fresh FOM, it is contained some sulfate radical in the surface area, but sulfate radical is disappeared in the modified-FOM (Table 2). Indeed, the specific surface area for modified-FOM exceeded that of fresh FOM. Fig. 2(a) and (b) display the SEM images of fresh and modified FOMs. The surface of modified FOM was rough with abundant protuberances and numerous pores, which favored the diffusion of the phosphate to its surface. Fig. 3 presents the XRD patterns of the Fe_3O_4 binary oxide in fresh and modified FOMs. The major peaks ($2\theta = 35$) were assigned to magnetite (Fe_3O_4) [22]. Since fresh and modified FOMs coated a layer of iron oxide on their surface, the XRD peak of Fe_3O_4 was very weak (Fig. 3(b) and (c)). X-ray energy dispersive analysis experiments were carried out to determine the composition of the magnetic product (Table 2). The SEM–EDS provides quantitative information on the surface of fresh and modified FOMs. The modified FOM contained 32.44 wt.% oxygen and 58.49 wt.% iron and fresh FOM contained 34.51 wt.% oxygen and 53.33 wt.% iron.

In Fig. 4, the modified FOM adsorbed more effectively than did the fresh FOM. Indeed, modified FOM is the best adsorbent herein and was therefore selected for use in subsequent experiments.

3.2. Effect of pH

Fig. 5 plots the effects of pH on phosphate adsorption. The results reveal that the pH is a significant parameter in the control of adsorption. The uptake of phosphate clearly increased as pH decreased, owing to the competition between the hydroxyl ions and the phosphate ions on the surface of the adsorbent [23].

The hydroxyl ions promoted the opposite reactions of those specified above, and so phosphate adsorption

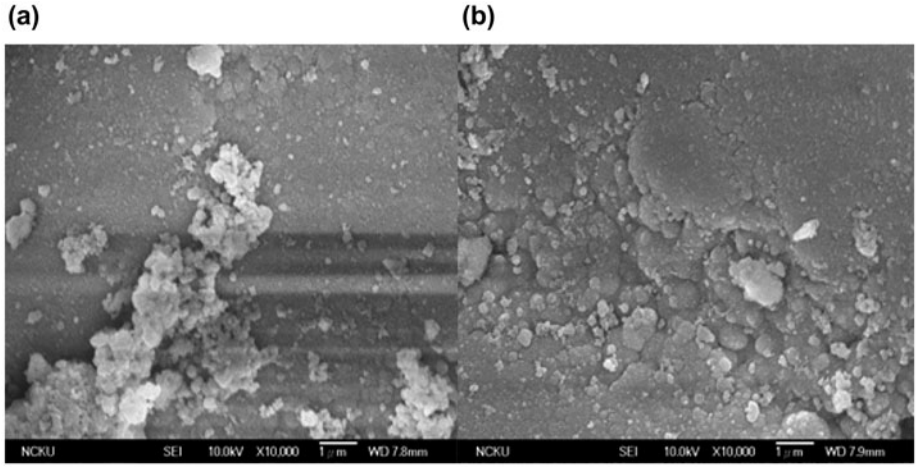

Fig. 2. The SEM of the FOM (a) fresh FOM, (b) modified FOM.

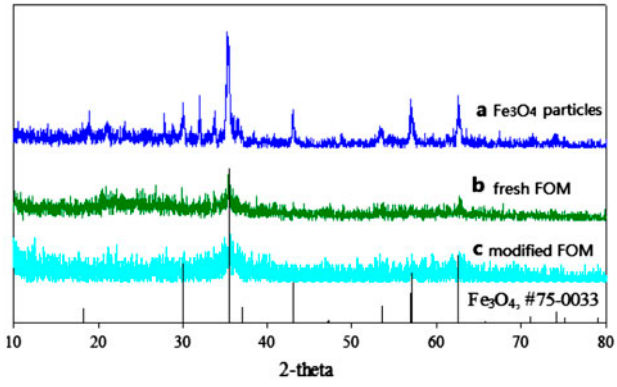

Fig. 3. XRD patterns for magnetite, fresh and modified FOMs (a) magnetic particles which were magnetized from the by-product of FBR-Fenton, (b) fresh FOM, (c) modified FOM.

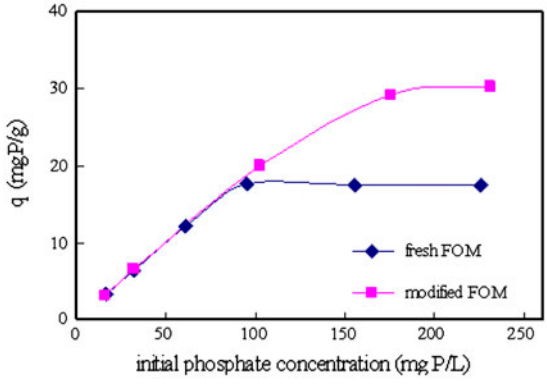

Fig. 4. The phosphate adsorption efficiency between fresh and modified FOMs.

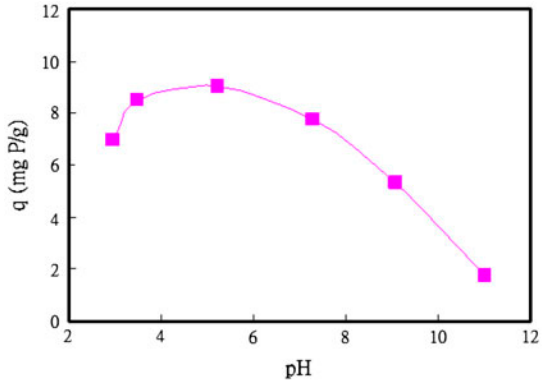

Fig. 5. The effect of pH on phosphate adsorption at 25°C (phosphate concentration 20.6 mg P/l, adsorbent dose = 2 g/l).

was poorer at higher pH. Accordingly, lower pH greatly favored adsorption. The adsorption capacity reached 9.8 mg P/g at pH 5, indicating that the FOM effectively adsorbs phosphate in an acidic environment.

3.3. Adsorption isotherms

The use of adsorption isotherms is a popular method for describing adsorption at a liquid/solid interface. A mathematical expression relates the concentration of adsorbate at the interface to its equilibrium concentration in the liquid phase. Langmuir and Freundlich models are used to describe the phosphate adsorption capacity of waste FOM. The Langmuir model is effective for describing the adsorption of a monolayer onto the surface of the adsorbent. All of the adsorption sites are equal and identical sites limited the adsorption capacity consistent with Eq. (1).

$$\frac{C_e}{q_e} = \frac{C_e}{q_m} + \frac{1}{K_L q_m} \quad (1)$$

where q_e and q_m are the amount and the maximum amount of adsorbed phosphate per unit weight of adsorbent (mg P/g), respectively; C_e denotes the residual concentration of adsorbate in the bulk solution (mg P/l), and K_L is a constant that is determined by plotting C_e/q_e against C_e.

The Freundlich model is commonly to describe multilayer absorption onto a surface with heterogeneous sites with various binding energies. The equation of the Freundlich model is as follows:

$$\log q_e = \log K_F + \frac{1}{n} \log C_e \quad (2)$$

K_F and $1/n$ are constants that are related to the adsorption of the adsorbent and the intensity of the adsorption, respectively. As presents in Fig. 6 and Table 3, the experimental data were better fitted by the Langmuir model than by the Freundlich model. The calculated maximum adsorption capacity is 30.8 mg P/g, which greatly exceeded the previously reported capacities of such adsorbents as iron oxide (12.6 mg P/g) [24], peat (8.91 mg P/g) [25], La-doped vesuvianite (6.7 mg P/g) [26], Fe Mn binary oxide (11.7 mg P/g) [27], MgMn double-layered hydroxides (7.3 mg P/g) [28], Fe-EDA-SAMMS (14.2 mg P/g) [29], hydrous niobium oxide (15 mg P/g) [18], and La/Al pillared montmorillonite (13.0 mg P/g) [20], providing evidence that FOM effectively adsorbs phosphate.

3.4. Adsorption kinetics of phosphate

In this study, the adsorption efficiencies of fresh FOM and modified FOM are evaluated. Fig. 7 plots the different amount of phosphate adsorbed onto the modified FOM against reaction time for different initial phosphate concentrations. The amount of phosphate adsorption increased with the initial phosphate concentration from 0.37 to 4.52 mM P/l. The amount of phosphate adsorbed became almost unchanged after 1,000 min of reaction.

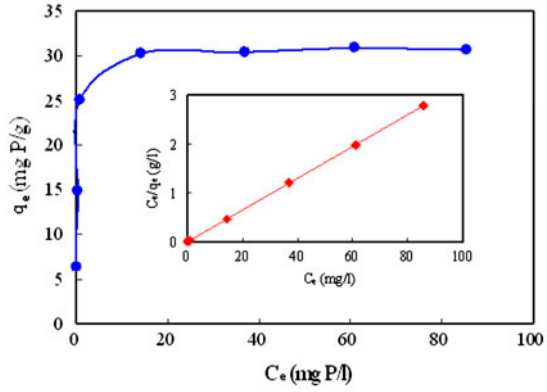

Fig. 6. Adsorption isotherm for phosphate on FOM at 25°C (P_i = 0.37–4.52 mM PO_4^{3-}/l, adsorbent dose = 1.8 g/l).

Table 3
Langmuir and Freundlich isotherm constants for the adsorption of phosphate ions on the modified FOM adsorbent

Langmuir			Freundlich		
q_m (mg/g)	K_L (l/mg)	R^2	n	K_F (l/mg)	R^2
30.8	6.77	0.999	0.26	1.15	0.920

A mathematical model, based on the Lagergren kinetic model, which specifies a pseudo-second-order kinetic model and was developed by Ho and McKay [30–32], was developed to explain the phosphate absorption rate curves. Based on this model, the reaction rate is expressed as follows:

$$\frac{dN_t}{dt} = k(N_e - N_t) \quad (3)$$

where the N_t is the number of occupied active sites on a sorbent, N_e is the number of sites available on the sorbent at equilibrium, and k is the pseudo-second-order rate constant. Based on the assumption that the quantity adsorbed is proportional to the number of active sites, Eq. (1) can be rewritten as,

$$\frac{dq_t}{dt} = k(q_e - q_t)^2 \quad (4)$$

where k is the sorption rate constant (g/mg min), q_e the amount of metal ions that is adsorbed at equilibrium (mg/g), and q_t is the amount of metal ions on the adsorbent surface at any time t (mg/g). Separating variables and integrating the equation for the initial limit, $t = 0$ and $q_t = 0$ yields,

$$\frac{1}{q_e - q_t} = \frac{1}{q_e} + kt \quad (5)$$

Eq. (5) is the integrated rate law for a pseudo-second-order reaction and can be rearranged into the following linear form.

$$\frac{t}{q_e} = \frac{1}{kq_e^2} + \frac{t}{q_e} \quad (6)$$

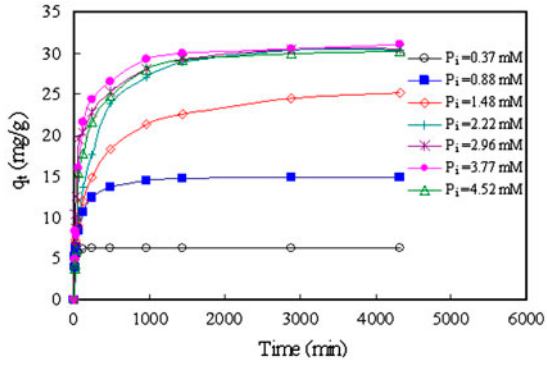

Fig. 7. Different amount of phosphate adsorption on the modified FOM with reaction time at different initial phosphate concentrations.

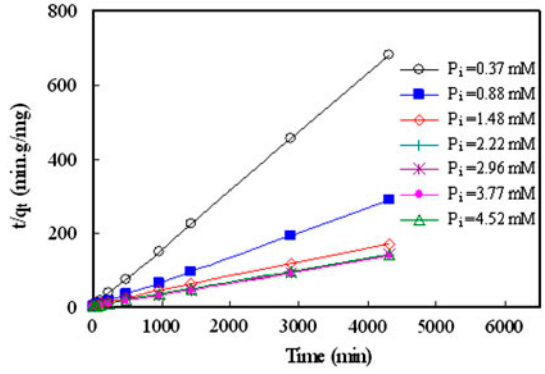

Fig. 8. Effect of phosphate concentration on the adsorption kinetics of phosphate ions by the modified FOM at pH 5 at temperature 25°C.

Based on Eq. (6), the values of q_e and K can be obtained from the slope $(1/q_e)$ and the intercept $(1/kq_e^2)$ of the straight line of t/q_t as a function of t. Fig. 8 plots t/q_t vs. t for the adsorption of phosphate onto iron ferrite and natural magnetite. The figure exhibits a linear relationship for both adsorbents. This linearity reveals that phosphate adsorption can be approximated by pseudo-second-order kinetics and the overall rate-constant appears to be controlled by the sorption mechanism as the adsorbent surface and adsorbate ions share or exchange electrons [33]. The equilibrium metal sorption, q_e, the rate constant, k, and the correlation coefficients, R^2, were calculated and presented in Table 4. Comparing the experimentally obtained sorption capacity, q_e, with values calculated using the model of Ho et al. [34] reveals close agreement, providing evidence of the pseudo-second-order kinetics. Fig. 8 displays the close fit of the pseudo-second-order model with the phosphate adsorption in the FOM. Table 4 presents the

Table 4
Different phosphate concentration for the adsorption of phosphate ions by modified FOM at various temperatures calculated from the second-order-rate constants

Initial P (mg/l)	$k \times 1{,}000$	q_e (exp) (mg/g)	q_e (cal) (mg/g)	R^2
11.5	41.0	6.3	6.3	1.0000
27.2	1.81	14.9	15.1	0.9999
45.9	0.37	25.1	25.4	0.9979
68.8	0.30	30.3	31.1	0.9987
91.7	0.62	30.5	30.8	0.9995
117.0	0.54	31.0	31.3	0.9997
140.9	0.40	30.7	31.3	0.9995

calculated value of q_e, which agrees closely with the experimental values in Fig. 8.

3.5. Thermodynamic parameters

The effect of temperature on the adsorption of phosphate ions by the FOM adsorbent is small, as presented in Fig. 9. Fig. 9 reveals that revealed the pseudo-second-order kinetic model is the best one for describing the adsorption of phosphate ions at various temperatures. Table 5 presents the kinetic parameters (k) and correlation coefficients (R^2), and plots of t/q_t vs. t at various temperatures in Fig. 10 are straight lines.

The rate constants (k) at various temperatures and the thermodynamic parameters for the adsorption process were evaluated. The activation energy (E_a) is obtained from an Arrhenius plot. The other activation parameters, including change in activation free energy (ΔG^*), change in activation enthalpy (ΔH^*) and change in activation entropy (ΔS^*), are calculated using the following equations [35,36].

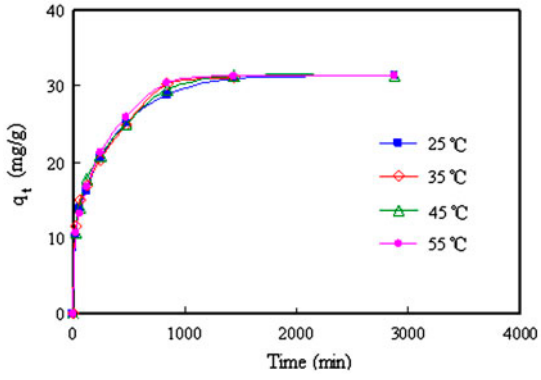

Fig. 9. Effect of temperature on the adsorption kinetics of phosphate ions by the modified FOM at pH 5 and an initial phosphate concentration of 5 mM.

Table 5
Thermodynamic parameters for the adsorption of phosphate ions by modified FOM at various temperatures calculated from the second-order-rate constants

T (℃)	E_a (kJ/mol)	$k \times 1{,}000$	R^2	ΔH (kJ/mol)	ΔG (kJ/mol)	ΔS (J/mol K)
25	2.7	0.36141	0.9979	−5.21	92.62	−328.29
35		0.39061	0.9976	−5.30	95.61	−327.62
45		0.39060	0.9980	−5.38	98.80	−327.61
55		0.40398	0.9981	−5.46	101.90	−327.32

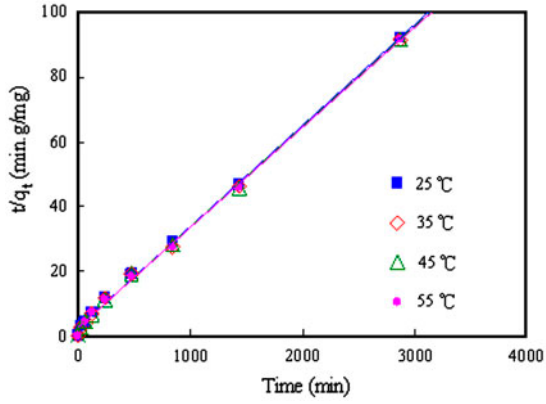

Fig. 10. The linear dependence of t/q on t by the modified FOM at pH 5 and an initial phosphate concentration of 5 mM P/l.

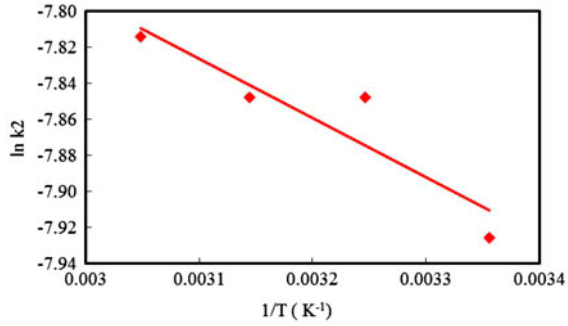

Fig. 11. Effect of temperature on the rate constant for the adsorption of Au(III) ions by the FOM adsorbent at pH 5 and an initial P ion concentration of 5 mM P/l.

$$\ln\ k_2 = \ln\ A - \frac{E_a}{RT} \tag{7}$$

$$k_2 = \frac{K_B T}{h} K^* \tag{8}$$

$$\Delta G^* = -RT\ \ln\ K^* \tag{9}$$

$$\Delta H^* = -E_a - RT \tag{10}$$

$$\Delta S^* = \frac{\Delta H^* - \Delta G^*}{T} \tag{11}$$

where E_a is the Arrhenius activation energy; A is the Arrenius factor; K_B and h are Boltzmann's and Planck's constants, respectively; R is the gas constant, and K^* is the equilibrium constant at temperature T. From Fig. 11, the slope of the linear plot of ln k_2 vs. $1/T$, which is the activation energy, is 2.7 kJ/mol. The activation energy of physisorption is 1–40 kJ/mol and that of chemisorption is 40–800 kJ/mol [37]. Indeed, the active energy of modified form is 2.7 kJ/mol which is less than 40 kJ/mol, the adsorption of phosphate ions on the modified FOM is fitted by physisorption.

Table 5 presents the activation energy and other thermodynamic parameters in transition state. The positive values of E_a, ΔG^*, ΔH^* indicate the presence of an energy barrier in the adsorption process. This is quite common and reasonable because the activated complex in the transition state is an excited form. Furthermore, the negative value of ΔS^* was resulted from the decreased randomness due to the adsorption of phosphate ions [38].

4. Conclusion

In this study, FOM that was generated from the by-product of an FBR-Fenton process was used as an adsorbent for treating phosphate wastewater. The BET surface area of modified FOM is 274.8 m^2/g, providing extensive open adsorption sites for phosphate removal. SEM observations revealed that FOM has a fractured and rough surface morphology. According to XRD analysis, FOM consists of a poorly crystallized magnetic phase in the form of iron oxide magnetic particles that are coated with iron oxide.

The adsorption isotherms, which are consistent with the Langmuir model, suggested that modified

FOM can be used for removing phosphate. Based on the Langmuir isotherms, the maximum phosphate adsorption capacity of modified FOM was 30.8 mg P/g (Table 4), which exceeded those of other adsorbents in the literature. Additionally, the adsorption process follows pseudo-second-order kinetics with a rate constant of approximately 4.1×10^{-2}–3×10^{-4} g/mg h at phosphate concentrations from 11.5 to 140.1 mg P/l. An activation energy of 2.7 kJ/mol is obtained for the physical adsorption. From the studies on the adsorption kinetics and thermodynamics of P ions, the calculated maximum adsorption capacity was 30.8 mg P/g which was much higher than previous reported. In the future, modified FOM will be an excellent adsorbent for practical use.

Acknowledgements

The authors thank financial supports from the Ministry of Economic Affairs of Republic of China for this research under Contract No. 101-EC-17-A-10-S1-187, and the Institute of Nuclear Energy Research (INER) under the Contract No. 1012001INER064. Ted Knoy is appreciated for his editorial assistance.

References

[1] K. Karageorgiou, M. Paschalis, G.N. Anastassakis, Removal of phosphate species from solution by adsorption onto calcite used as natural adsorbent, J. Hazard. Mater. 139 (2007) 447–452.
[2] C. McComas, D. McKinley, Reduction of phosphorus and other pollutants from industrial dischargers using pollution prevention, J. Clean. Prod. 16 (2008) 727–733.
[3] C.W. Lee, H.B. Kwon, H.P. Jeon, B. Koopman, A new recycling material for removing phosphorus from water, J. Clean. Prod. 17 (2009) 683–687.
[4] L.E. de-Bashan, Y. Bashan, Recent advances in removing phosphorus from wastewater and its future use as fertilizer (1997–2003), Water Res. 38 (2004) 4222–4246.
[5] G. Morse, S. Brett, J. Guy, J. Lester, Review: Phosphorus removal and recovery technologies, Sci. Total Environ. 212 (1998) 69–81.
[6] M. Rafatullah, O. Sulaiman, R. Hashim, A. Ahmad, Adsorption of methylene blue on low-cost adsorbents: A review, J. Hazard. Mater. 177 (2010) 70–80.
[7] S. Asaoka, T. Yamamoto, Characteristics of phosphate adsorption onto granulated coal ash in seawater, Mar. Pollut. Bull. 60 (2010) 1188–1192.
[8] J. Chen, H. Kong, D. Wu, Z. Hu, Z. Wang, Y. Wang, Removal of phosphate from aqueous solution by zeolite synthesized from fly ash, J. Colloid Interface Sci. 300 (2006) 491–497.
[9] M.Y. Can, E. Yildiz, Phosphate removal from water by fly ash: Factorial experimental design, J. Hazard. Mater. 135 (2006) 165–170.
[10] E. Yildiz, Phosphate removal from water by fly ash using crossflow microfiltration, Sep. Purif. Technol. 35 (2004) 241–252.
[11] Y. Xue, H. Hou, S. Zhu, Characteristics and mechanisms of phosphate adsorption onto basic oxygen furnace slag, J. Hazard. Mater. 162 (2009) 973–980.
[12] E. Oguz, Removal of phosphate from aqueous solution with blast furnace slag, J. Hazard. Mater. 114 (2004) 131–137.
[13] C.-J. Liu, Y.-Z. Li, Z.-K. Luan, Z.-Y. Chen, Z.-G. Zhang, Z.-P. Jia, Adsorption removal of phosphate from aqueous solution by active red mud, J. Environ. Sci. 19 (2007) 1166–1170.
[14] Y. Li, C. Liu, Z. Luan, X. Peng, C. Zhu, Z. Chen, Z. Zhang, J. Fan, Z. Jia, Phosphate removal from aqueous solutions using raw and activated red mud and fly ash, J. Hazard. Mater. 137 (2006) 374–383.
[15] G. Akay, B. Keskinler, A. Cakici, U. Danis, Phosphate removal from water by red mud using crossflow microfiltration, Water Res. 32 (1998) 717–726.
[16] Y. Yang, Y. Zhao, A. Babatunde, L. Wang, Y. Ren, Y. Han, Characteristics and mechanisms of phosphate adsorption on dewatered alum sludge, Sep. Purif. Technol. 51 (2006) 193–200.
[17] S. Lee, B. Choi, K. Kim, Removal of phosphate by seafood processing wasted sludge, Water Sci. Technol. 46 (2002) 297–302.
[18] L.A. Rodrigues, M.L.C.P. da Silva, Thermodynamic and kinetic investigations of phosphate adsorption onto hydrous niobium oxide prepared by homogeneous solution method, Desalination 263 (2010) 29–35.
[19] M.X. Zhu, K.Y. Ding, S.H. Xu, X. Jiang, Adsorption of phosphate on hydroxyaluminum- and hydroxyiron-montmorillonite complexes, J. Hazard. Mater. 165 (2009) 645–651.
[20] S. Tian, P. Jiang, P. Ning, Y. Su, Enhanced adsorption removal of phosphate from water by mixed lanthanum/aluminum pillared montmorillonite, Chem. Eng. J. 151 (2009) 141–148.
[21] Y.H. Huang, Y.J. Shih, C.C. Chang, Adsorption of fluoride by waste iron oxide: The effects of solution pH, major coexisting anions, and adsorbent calcination temperature, J. Hazard. Mater. 186 (2011) 1355–1359.
[22] Y. Feng, J.-L. Gong, G.-M. Zeng, Q.-Y. Niu, H.-Y. Zhang, C.-G. Niu, J.-H. Deng, M. Yan, Adsorption of Cd(II) and Zn(II) from aqueous solutions using magnetic hydroxyapatite nanoparticles as adsorbents, Chem. Eng. J. 162 (2010) 487–494.
[23] H. Liu, X. Sun, C. Yin, C. Hu, Removal of phosphate by mesoporous ZrO_2, J. Hazard. Mater. 151 (2008) 616–622.
[24] L. Zeng, X. Li, J. Liu, Adsorptive removal of phosphate from aqueous solutions using iron oxide tailings, Water Res. 38 (2004) 1318–1326.
[25] J.B. Xiong, Q. Mahmood, Adsorptive removal of phosphate from aqueous media by peat, Desalination 259 (2010) 59–64.
[26] H. Li, J. Ru, W. Yin, X. Liu, J. Wang, W. Zhang, Removal of phosphate from polluted water by lanthanum doped vesuvianite, J. Hazard. Mater. 168 (2009) 326–330.
[27] G. Zhang, H. Liu, R. Liu, J. Qu, Removal of phosphate from water by a Fe–Mn binary oxide adsorbent, J. Colloid Interface Sci. 335 (2009) 168–174.
[28] R. Chitrakar, S. Tezuka, A. Sonoda, K. Sakane, K. Ooi, T. Hirotsu, Adsorption of phosphate from seawater on calcined MgMn-layered double hydroxides, J. Colloid Interface Sci. 290 (2005) 45–51.
[29] W. Chouyyok, R.J. Wiacek, K. Pattamakomsan, T. Sangvanich, R.M. Grudzien, G.E. Fryxell, W. Yantasee, Phosphate removal by anion binding on functionalized nanoporous sorbents, Environ. Sci. Technol. 44 (2010) 3073–3078.
[30] E. Oguz, Sorption of phosphate from solid/liquid interface by fly ash, Colloids Surf., A: Physicochem. Eng. Asp. 262 (2005) 113–117.
[31] M.S. Onyango, Y. Kojima, H. Matsuda, A. Ochieng, Adsorption kinetics of arsenic removal from groundwater by iron-modified zeolite, J. Chem. Eng. Jpn. 36 (2003) 1516–1522.
[32] Y.S. Ho, G. McKay, The kinetics of sorption of divalent metal ions onto *Sphagnum* moss peat, Water Res. 34 (2000) 735–742.
[33] V.C. Taty-Costodes, H. Fauduet, C. Porte, A. Delacroix, Removal of Cd(II) and Pb(II) ions, from aqueous solutions, by adsorption onto sawdust of *Pinus sylvestris*, J. Hazard. Mater. 105 (2003) 121–142.
[34] Y. Ho, G. McKay, Pseudo-second order model for sorption processes, Process Biochem. 34 (1999) 451–465.

[35] R.S. Juang, F.C. Wu, R.L. Tseng, The ability of activated clay for the adsorption of dyes from aqueous solutions, Environ. Technol. 18 (1997) 525–531.
[36] W. Stumm, J.J. Morgan, Aquatic Chemistry: An Introduction Emphasizing Chemical Equilibria in Natural Waters, second ed., J. Wiley & Sons, New York, NY, 1981.
[37] R.M. Cornell, U. Schwertmann, The Iron Oxides: Structure, Properties, Reactions, Occurrences, and Uses, second ed., Wiley-VCH, New York, NY, 2003.
[38] Y.-C. Chang, D.-H. Chen, Recovery of gold(III) ions by a chitosancoated magnetic nano-adsorbent, Gold Bull. 39 (2006) 98–102.